Chin. Geogra. Sci. 2015 Vol. 25 No. 6 pp. 765–774
doi: 10.1007/s11769-014-0716-z

Springer Science Press
www.springerlink.com/content/1002-0063

Simulating Evolution of a Loess Gully Head with Cellular Automata

LIU Xiaojing, TANG Guo′an, YANG Jianyi, SHEN Zhou, PAN Ting

(*School of Geography Science*, *Nanjing Normal University*, *Nanjing* 210046, *China*)

Abstract: This paper presents a new method for simulating the evolution of a gully head in a loess catchment with cellular automata (CA) based on the Fisher discriminant. The experimental site is an indoor loess catchment that was constructed in a fixed-intensity rainfall erosion test facility. Nine high-resolution digital elevation model (DEM) data sets were gathered by close range photogrammetry during different phases of the experiment. To simulate the evolution of the catchment gully head, we assumed the following. First, the 5th and 6th DEM data sets were used as a data source for acquiring the location of the catchment gully head and for obtaining spatial variables with GIS spatial analysis tools. Second, the Fisher discriminant was used to calculate the weight of the spatial variables to determine the transition probabilities. Third, CA model was structured to simulate the evolution of the gully head by iterative looping. The status of the cell in the CA models was dynamically updated at the end of each loop to obtain realistic results. Finally, the nearest neighbor, G-function, K-function, Moran′s I and fractal indexes were used to evaluate the model results. Overall, the CA model can be used to simulate the evolution of a loess gully head. The experiment demonstrated the advantages of the CA model which can simulate the dynamic evolution of gully head evolution in a catchment.

Keywords: cellular automata; digital elevation model (DEM); gully head; loess catchment; point pattern

Citation: Liu Xiaojing, Tang Guo′an, Yang Jianyi, Shen Zhou, Pan Ting, 2015. Simulating evolution of a loess gully head with cellular automata. *Chinese Geographical Science*, 25(6): 765–774. doi: 10.1007/s11769-014-0716-z

1 Introduction

The Loess Plateau in the north of China is famous for its deep loess (Shi and Shao, 2000). Due to the special geographic landscape, soil and climatic conditions, and long history (over 5000 years) of human activity, there has been intensive soil erosion which has resulted in prolonged and great impacts on social and economic development in the region (Shi and Shao, 2000). The small loess watershed is the basic unit for managing the ecological environment in the Loess Plateau, and its evolution is a snapshot of terrain development in the loess region (Cao *et al*., 2013). Thus, it is critical to understand terrain evolution in small loess watersheds.

Several studies have been focused on using math to construct landform evolution models based on digital elevation model (DEM). These models include the erosional development of catchments and their networks (Willgoose *et al.*, 1991), a nonlinear, two-dimensional landscape evolution model (Tucker and Slingerland, 1994), drainage basin evolution model (Howard, 1994), topographic evolution model (Densmore *et al*., 1998) and the mathematically whole-landscape evolution model (Willgoose, 2005). However, due to the complexity of evolution in the loess landform process, it is difficult and time consuming to predict the evolution of the loess landform based on traditional mathematical formulas that predict the quantity and rate of runoff and sediment. Thus, the cellular automata (CA) was proposed as a method for simulating landform evolution to

Received date: 2013-04-09; accepted date: 2013-07-17
Foundation item: Under the auspices of National Natural Science Foundation of China (No. 41171320, 41101349), National Innovation and Entrepreneurship Program (No. 201210319025)
Corresponding author: TANG Guo′an. E-mail: tangguoan@njnu.edu.cn

overcome the disadvantages of traditional methods.

The CA is a discrete, spatio-temporal, local dynamics model. The micro-local interactions of individual cells in the CA are used to build macro-scale patterns (Gregorio and Serra, 1999). Currently, CA has successfully been applied to urban expansion and population dynamics (Couclelis, 1985; 1988; 1989), wildfire diffusion (Clarke *et al*., 1994; Hargrove *et al*., 2000), landscape changes (Wang and Zhang, 2001), urban evolution (Clarke *et al*., 1997; Couclelis, 1997; Batty *et al*., 1999; Li and Yeh, 2000; Wu, 2002; Li and Liu, 2006; Liu *et al*., 2008a; 2008b; 2014; Yang *et al*., 2013) and land-use changes (White and Engelen, 1993; Clarke and Gaydos, 1998; Wu and Webster, 1998; Li and Yeh, 2002; Liu *et al*., 2010). The CA also has been used for landform evolution (Smith, 1991; Chase, 1992; Murray and Pola, 1994; Ke, 2006; Tian *et al*., 2008; Cao *et al*., 2013). These studies have demonstrated the capability of CA for simulating and predicting complex geographical processes. However, few studies simulated the evolution of gully heads in loess watersheds. Gully head is one of important features of gully. The position and shape of the gully heads and their width and depth can be used to determine the activity and morphological characteristics of gullies (Zucca *et al*., 2006). Through imitating the evolution of gully heads, the development of small loess watershed can be known roughly, which is helpful to understand terrain evolution in small loess watersheds. This study applied CA for simulating the evolution of a loess catchment gully head in a small indoor loess watershed with artificial rainfall.

2 Materials and Methods

2.1 Experimental data

An indoor loess catchment was constructed in the rainfall erosion test facility at the State Key Laboratory of Soil Erosion and Dryland Farming on the Loess Plateau in China. This catchment covers an area of 31.49 m^2 with a maximum length, width, circumference, and valley height difference of 9.1 m, 5.8 m, 23.3 m, and 3.15 m, respectively. This small catchment is filled with loess soil at a bulk density of 1.39 g/cm^3. The soil was obtained from the top layer of a loess field in the Yangling Agricultural High Tech Industries Demonstration Zone (34°12′00″N, 108°25′48″E) in Shaanxi Province, China.

The catchment was monitored by collecting low-altitude and close-range digital images under artificially designed rainfall. Nine high-resolution DEM data sets (Fig. 1) were gathered with close range photogrammetry during different experimental phases with a revolution of 10 mm and mean-square-error of 2 mm (based on the stereo images). The time interval between the two photography events was approximately 1 week. During each period, 2–5 artificial rainfalls occurred. More specific parameters are shown in Table 1. The changes of DEMs

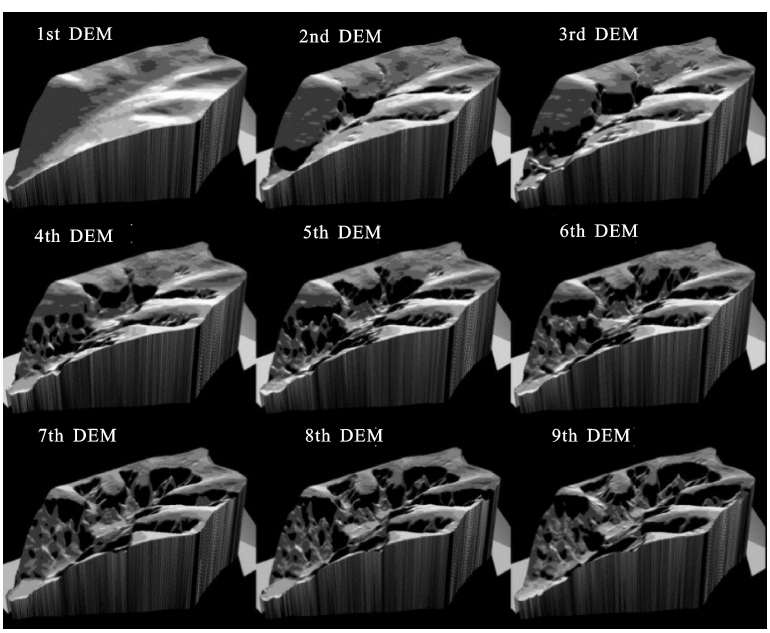

Fig. 1 Nine high-resolution digital elevation model (DEM) data sets

Table 1 Rainfall and photography characteristics in artificially simulated rainfall conditions

Rainfall event (Photography event)	Rainfall date (Photography date)	Designed rainfall intensity (mm/min)	Measured rainfall intensity (mm/min)	Duration of rainfall (min)	Quantum of rainfall (mm)
(First period)	(2001-07-29)	0.00[a]	0.00[a]	0.00[b]	0.000[b]
1	2001-07-30	0.50	0.54	90.50	48.915
2	2001-08-01	0.50	0.52	89.50	46.540
3	2001-08-03	0.50	0.49	89.50	63.939
4	2001-08-05	1.00	1.18	47.52	65.050
5	2001-08-08	1.00	1.21	45.86	73.580
(Second period)	(2001-08-13)	0.70[a]	0.79[a]	362.88[b]	298.024[b]
6	2001-08-14	2.00	2.41	30.53	53.750
7	2001-08-17	1.00	1.19	46.17	51.528
(Third period)	(2001-08-19)	1.50[a]	1.80[a]	76.80[b]	105.278[b]
8	2001-08-20	0.50	0.57	90.18	36.167
9	2001-08-22	0.50	0.59	61.95	55.704
(Fourth period)	(2001-08-27)	0.50[a]	0.58[a]	152.13[b]	91.871[b]
10	2001-08-28	1.00	1.20	47.92	65.360
11	2001-08-31	2.00	2.15	31.17	65.360
(Fifth period)	(2001-09-01)	1.50[a]	1.78[a]	79.09[b]	130.720[b]
12	2001-09-03	0.50	0.52	62.94	31.896
13	2001-09-05	0.50	0.58	61.53	35.960
14	2001-09-07	0.50	0.56	60.83	34.290
(Sixth period)	(2001-09-11)	0.50[a]	0.55[a]	185.30[b]	102.146[b]
15	2001-09-11	1.00	1.12	46.82	52.438
16	2001-09-14	1.00	1.08	45.83	49.896
17	2001-09-17	1.00	0.98	47.02	45.256
18	2001-09-20	1.00	1.04	45.37	47.180
(Seventh period)	(2001-09-21)	1.00[a]	1.04[a]	185.04[b]	194.770[b]
19	2001-09-24	2.00	2.12	30.37	64.384
20	2001-09-27	2.00	1.98	34.35	67.736
(Eighth period)	(2001-09-28)	2.00[a]	2.05[a]	64.72[b]	132.120[b]
21	2001-09-30	0.50	0.53	91.27	48.373
22	2001-10-09	0.50	0.55	90.60	49.83
23	2001-10-11	0.50	0.60	89.72	53.832
(Ninth period)	(2001-10-12)	0.50[a]	0.56[a]	271.59[b]	152.035[b]

Notes: a, mean value; b, total. Photography characteristics are in the parentheses
Source: Cui, 2002

revealed the developments of gully. The 5th and 6th sets of DEM were chosen to determine the location of the catchment gully heads and extract spatial variables, because the two sets had most obvious gully development.

2.2 Methods

2.2.1 Fisher discriminant based CA for calculating transition probabilities

Traditional CA methods can not easily handle complex variables or determine parameter values (Li and Yeh, 2002). The basic Fisher discriminant method projects multidimensional data in one direction. Then, the points of the same class will gather and the points of different classes will separate. With this method, it is easy to deal with the complex relationships that occur between spatial variables and with the evolution of loess catchment gully heads. The contribution of each spatial variable to the simulation is quantified by its associated weight or

parameter.

In the CA model, the cell status is 0 or 1. In this case, ′0′ indicates that the cell is not a gully head and ′1′ indicates that the cell is a gully head. This simulation assumes that a relationship exists between the status (a gully head or not a gully head) and the transition probability. The transition probability can be expressed as follows (Liu and Li, 2007):

$$P_{is}(i,j)=\frac{\exp(U_{is}(i,j))}{\exp(U_{is}(i,j))+\exp(U_{not}(i,j))} \quad (1)$$

where $P_{is}(i, j)$ is the transition probability of the cell $\{i, j\}$; and $U_{is}(i, j)$ and $U_{not}(i, j)$ are two discriminants that are calculated based on the spatial variables of the Fisher discriminant as follows:

$$\begin{cases} U_{is}(i,j)=\sum_{i=1}^{k} a_{is_i} X_i(i,j)+a_{is} \\ U_{not}(i,j)=\sum_{i=1}^{k} a_{not_i} X_i(i,j)+a_{not} \end{cases} \quad (2)$$

where $U_{is}(i, j)$ is discriminant of transition; $U_{not}(i, j)$ is discriminant of no transition, X_i $(1 \le i \le k)$ are spatial variables that affect the evolution of the catchment gully head; and i means different categories of X. In addition. a_{is} are the weight vectors of spatial variables in the case of transition, a_{not} are in the case of no transition.

It is appropriate to scale spatial variables as Fisher discriminant input data. Converting input data to a range of [0, 1] can eliminate the differences between the data ranges of various spatial variables. Scaling each variable allows them to be treated as variables in the Fisher discriminant (Liu and Li, 2007). Transformations were conducted as follows:

$$x'=\frac{x-x_{min}}{x_{max}-x_{min}} \quad (3)$$

where x' are the scaled data; ; x are the input data; and x_{max} and x_{min} are the maximum and minimum of x.

A series of unknown or uncertainty factors occur during the simulation of the catchment gully head evolution. Therefore, a stochastic disturbance factor must be introduced. The transition probability was revised as follows:

$$p\{i, j\} = A \times P_{is}(i, j) \quad (4)$$

where $p\{i, j\}$ is the final transition probability of cell $\{i, j\}$; $P_{is}(i, j)$ is the initial value of transition probability without considering the disturbance factor; and A is stochastic disturbance which reflects a series of unknown or uncertain factors during simulation. The value of A should be integrated with experience means.

2.2.2 Transition rules and model structures

It is important to structure transition rules for the CA model. Cells with a status of 1 are called gully head cells. Gully head cells should be identified first. Next, the cells with transition probabilities with a maximum of 3 × 3 near the gully head cells are identified as potential gully head cells. The elevation of the potential gully head cell should be greater than the current elevation of the gully head cell. To control the conversion rate, the potential gully heads must be arranged according to their transition probabilities. In addition, only top R% of the potential gully head cells can be transformed into new gully heads in this iteration. A suitable R-value (e.g., 0.85) is useful for obtaining adequate simulation results. After one iteration, the status of cells will be changed. New gully head cells will replace the old gully cells. Simultaneously, the old gully cells will be flagged to avoid changing them in the next iteration. The cell status in the CA model is dynamically updated at the end of each loop to make the simulation results more realistic.

3 Implementation

3.1 Extraction of gully head

The gully head is defined as where the slope is low but changes deeply. Thus, the gully head is defined as where the slope variation (SOS) is large and the slope is small (Fig. 2). The 5th and 6th DEMs were used as data sources and the ArcGIS analysis tools were used to define the 5th and 6th gully head locations in the catchment (Fig. 3). The gully head data were converted into raster format in which each cell represents an area of

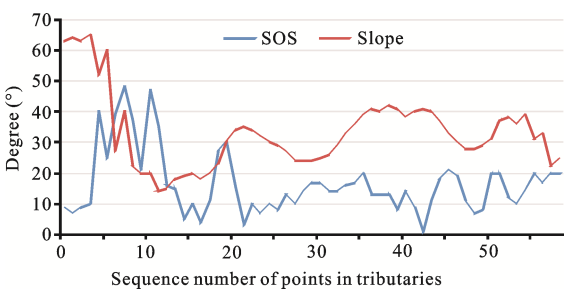

Fig. 2 Slope gradient and slope variations in tributaries. SOS, slope variation

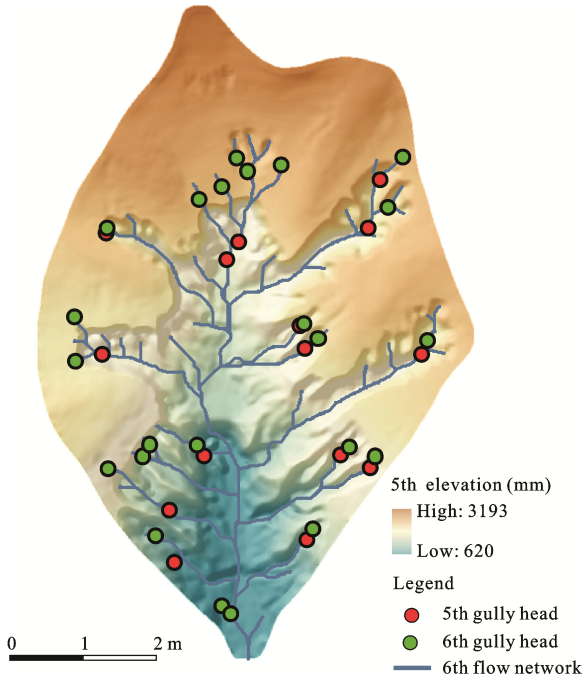

Fig. 3 The 5th and 6th catchment gully head location

10 mm × 10 mm in the catchment. Each cell is given only one status (0 or 1). A status of ′0′ indicates that the cell is not a gully head and a status of ′1′ indicates that the cell is a gully head. The 5th catchment gully head provides the initial cell status and the 6th catchment gully head provides the actual cell status that is ideal for the simulation model.

3.2 Transition probability calculations

Many factors affect loess erosion processes, including rainfall runoff, geomorphic conditions, soil corrosion resistance, vegetation, and human activities. The catchment in this study was subjected to artificial rainfall of fixed intensity. In this case, the gully head transition usually resulted from a series of spatial topographic or distance variables, including slope and the distance of each cell from the gully edge. Here, ArcGIS was used to obtain the spatial variables that were used in the simulation (Table 2).

The sample function in ArcGIS was used to determine the locations of the random samples and the values of the spatial variables. Random samples should include both gully head units and potential gully head units. The Fisher discriminant function of the SPSS was used to calculate the Fisher discriminant parameters. The outputs of the Fisher discriminants are as follows:

$$\begin{cases} U_{\text{is}} = 48.549 \times DEM + 83.538 \times DISTANCE - 11.142 \times FLOWACC + 3.532 \times ASPECT + 14.335 \times SOA + 4.606 \times SURFACEINCISION - 29.964 \times RELIEFAMPLITUDE + 40.103 \times SLOPE - 28.487 \\ U_{\text{not}} = 40.742 \times DEM + 87.171 \times DISTANCE - 7.347 \times FLOWACC + 7.752 \times ASPECT + 17.815 \times SOA - 1.951 \times SURFACEINCISION - 19.741 \times RELIEFAMPLITUDE + 34.277 \times SLOPE - 27.187 \end{cases} \quad (5)$$

where *DEM*, *DISTANCE*, *FLOWACC*, *ASPECT*, *SOA*, *SURFACEINCISION*, *RELIEFAMPLITUDE*, *SLOPE* are spatial variables that affect the evolution of the catchment gully head. The descriptions of these spatial variables are shown in Table 2.

Table 2 Spatial variables, their descriptions and acquiring methods

Spatial variable	Description	Acquiring method
ASPECT	Slope direction or compass direction of a hill	ArcGIS/Aspect Tool
FLOWACC	Sum of accumulated flow to each cell	ArcGIS/Hydrological Analysis
SLOPE	Steepest downhill slope for a location on a surface	ArcGIS/Slope Tool
SLENGTH	Horizontal distance from origin of overland flow to center point of each cell	ArcGIS/Slope Length Tool
DISTANCE	Distance from gully edge to each cell	ArcGIS/Euclidean Distance Tool
DEM	Elevation	Fifth DEM initial data
SOS	Changes in slope	ArcGIS/Slope Tool
SOA	Changes in aspect	ArcGIS/Aspect and Slope Tool
RELIEFAMPLITUDE	Height difference between maximum and minimum elevation for a specific area	ArcGIS/Neighborhood Tool
ROUGHNESS	Initial simulated terrain roughness	Ratios of surface area to projection area
SURFACEINCISION	Height difference between average and minimum elevation for a specific area	ArcGIS/Neighborhood Tool

The calculated values of $U_{is}(i, j)$ and $U_{not}(i, j)$ should be put in equations (2) and (4) to obtain the transition probabilities. Cells with higher calculated values have a greater conversion probability.

3.3 Simulation of gully head evolution

The dynamic catchment gully head evolution process was simulated based on the calculated transition probabilities and conversion rules. When no potential gully head cell was found around just one gully head cell, the iteration was stopped. The initial status of this simulation is the 5th catchment gully head. The 30 iteration loops were conducted and only 85% of the potentially changed cells were altered during each iterative process to control the conversion rate.

4 Simulation Results and Discussion

The simulated results are shown in Fig. 4. In addition, the spatial overlay between the simulated gully head and the river network was used to simulate the evolution process dynamically as the gully head extends towards the river network. This study evaluated the simulated results from three aspects, including 1) spatial point pattern, 2) spatial autocorrelation, and 3) fractal dimension.

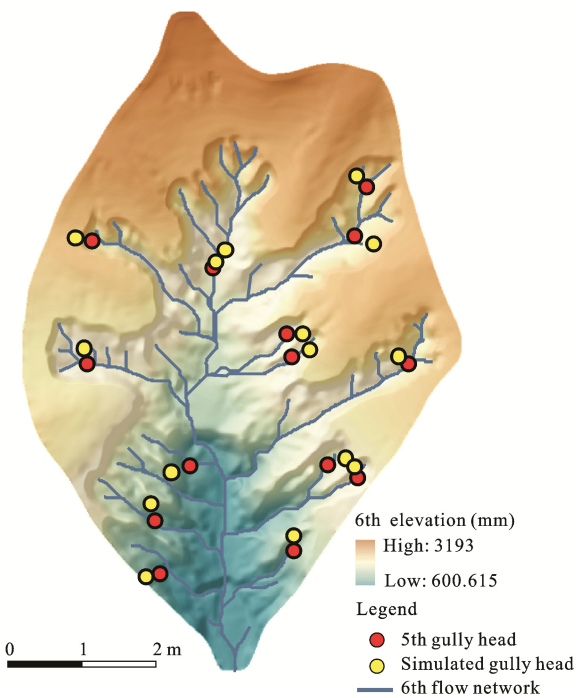

Fig. 4 Simulated results

4.1 Spatial point pattern

The analysis of spatial point patterns came to prominence in geography during the late 1950s and early 1960s (Gatrell *et al*., 1996). One method that was used to analyze spatial point patterns was the distance-based technique, using information on the spacing of the points to characterize pattern (typically, mean distance to the nearest neighboring point) (Gatrell *et al*., 1996). In this study, distance-based techniques which include the nearest neighbor, G-function, and K-function techniques, were applied to evaluate the simulated results.

The nearest neighbor index was applied to calculate the mean distance to the nearest neighboring point and to compare the similarities of the mean distances between the observed and expected data. Here, the nearest neighbor index was calculated as the ratio of the mean distance to the nearest neighboring gully head of the simulated result to the expected value of the actual gully head. The nearest neighbor index (R) in this study was calculated as follows (Clark and Evans, 1954):

$$R = \frac{\overline{d_{\min}}}{\overline{D_{\min}}} \tag{6}$$

where R is the nearest neighbor index; and $\overline{d_{\min}}$ and $\overline{D_{\min}}$ are the mean distances to the nearest neighboring points of the simulated and actual gully head, respectively. The value was calculated with the following equation:

$$\overline{d_{\min}} = \frac{1}{n}\sum_{i=1}^{n} d_{\min}(S_i) \tag{7}$$

where S_i represents the ith gully head; n is the total number of gully heads; and $d_{\min}(S_i)$ is the distance from the ith gully head to its nearest neighbor.

The calculated results are presented in Table 3. Next, the F-test was used to determine if the model results were statistically significant. The null hypothesis is rejected if the F calculated from the data is greater than the critical value of the F-distribution for some desired false-rejection probability (e.g., 0.05). Otherwise, the null hypothesis is not rejected and the variables are not statistically significant. In this experiment, F = 1.169. Looking up the F distribution table, 0.05 critical value for an F distribution with 1 and 40 degrees of freedom is $F_{0.05}(1, 40)$ ($F_{0.05}(1, 40)$ = 7.31). Since $F < F_{0.05}(1, 40)$,

it is accepted that simulated result is of the same spatial pattern with actual gully head.

However, just using mean distance to the nearest neighboring gully head to describe its spatial pattern is not appropriate, because this method ignores the distribution of nearest neighbor distances. The G-function is introduced to resolve this limitation and assembles the complete cumulative probability distribution of the point to the point nearest neighbor distances as a function of distance, d (Unwin, 1996).

$$G(d) = \frac{\#(d_{\min}(S_i) \le d)}{n} \tag{8}$$

where # indicates the number of events that $d_{\min}(S_i)$ is less than or equal to d; and n is the total number of $d_{\min}(S_i)$.

The results of actual and simulated gully head G-Function can be found in Fig. 5. Simulated gully head and actual gully head have a common trend, which indicates they are of the same spatial pattern regarding the aspect of the first-order point pattern behaviors.

However, the G-function is a method for characterizing the first-order behavior of a point pattern. This function only considers the nearest distance of the process across space. The nearest neighbor method and the G-function can only test for the presence of a pattern on a single scale (Ripley, 1977). To study the correlations between the process values at different regions in space, Ripley (1977) proposed the K-function. The K-function uses the second-order analysis of point patterns in a two-dimensional space. If a point process is stationary and isotropic, there is a close mathematical relationship between the second-order intensity and an alternative characterization of second-order properties known as the K function (Ripley, 1977; Haase, 1995).

The actual and final gully head simulations were used in the ArcGIS Multi-Distance Spatial Cluster Analysis (Ripleys K Function) Tool (Fig. 6). Simulated gully head and actual gully head have a common trend in Fig. 6, which indicates they are of the same spatial pattern regarding the aspect of the second-order point pattern behaviors.

4.2 Spatial autocorrelation

In statistics, Moran′s I is a measure of the spatial autocorrelation developed by Patrick A P Moran (Moran, 1950). Spatial autocorrelation is characterized by the correlation of a signal among its nearby locations in space. The Moran′s I parameter is a weighted correlation coefficient that is used to detect departures from spatial randomness (Moran, 1950). In addition, the spatial randomness is used to determine whether neighboring areas are more similar than expected according to the null hypothesis.

A software called GEODA was used to calculate the Moran′s I parameter of the simulated and actual gully head results (Table 3). The calculated results demonstrated that the two gully heads follow a clustering distribution. However, some differences occurred between the simulated and actual gully head results comparing the Moran′s I.

4.3 Fractal dimension

The fractal dimension is an index that characterizes the fractal pattern or set by quantifying complexity as a ratio of detail changes to scale changes (Mandelbrot, 1983). Here, the fractal dimension method was used to calculate the fractal index D for the actual and simulated gully heads to characterize the point distribution. Two different methods for calculating fractal geometry were introduced, including 1) the box-counting method (Neil and Curtis, 1997), and 2) the scale transformation.

(1) The box-counting method. A serious of grids composed of squares with uniform side lengths ε was created. The number of boxes of size ε that contain at

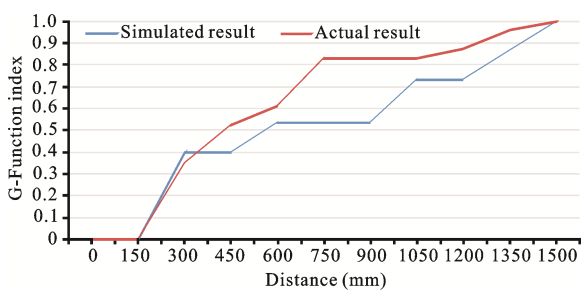

Fig. 5 Result of actual and simulated gully head G-Function index

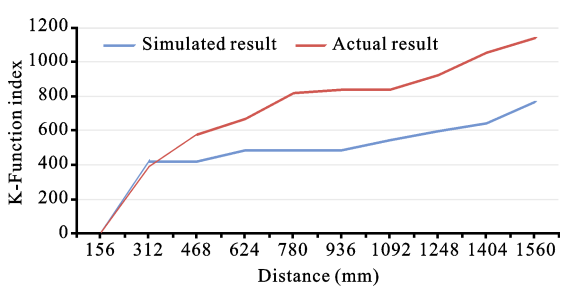

Fig. 6 Result of actual and simulated gully head K-Function index

least one gully head was recorded as $N(\varepsilon)$. When the size of the boxes decreases the $N(\varepsilon)$ value increases. The value of D was estimated by the following equation:

$$\lg N(\varepsilon) = -D\lg\varepsilon + A \quad (9)$$

where ε are side lengths of squares; $N(\varepsilon)$ is the number of boxes of size ε that contain at least one gully head. Next, a graph of $\lg N(\varepsilon)$ vs. $\lg\varepsilon$ was produced for the actual and simulated points. The correlation between $N(\varepsilon)$ and ε was adjusted by linear regression and the slope of the straight line was used as the index D (Table 3).

(2) The scale transformation. Based on the Box-counting method, the grids were changed to circles. The center of the circle represents the center of points and the number of points that are covered by the circle of radius λ was recorded. When the radius decreases the $N(\lambda)$ value decreases. The value of D was estimated by the following equation:

$$\lg N(\lambda) = D\lg\lambda + A \quad (10)$$

A graph of $N(\lambda)$ vs. $\lg\lambda$ for the actual and simulated points was produced. Next, the correlation between $N(\varepsilon)$ and ε was adjusted by linear regression and the slope of the line was used as the index D (Table 3). The correlation coefficient represents the interdependence of $N(\lambda)$ and $\lg\lambda$ and the index D reflects the spatial distribution of the gully head.

The nearest neighbor, G-function, K-function, Moran′s I and fractal index D were chosen to prove that a suitable match occurred between the actual and simulated gully heads regarding the point spatial pattern, the spatial autocorrelation and the fractal dimension. The simulation resulted in consistent spatial distribution. All of these comparisons demonstrated the validity of the the Fisher discriminant based CA model.

5 Conclusions

The CA models have become a useful tool for simulating and predicting complex geographical processes. Simulation of gully head evolution is not only theoretically important but also of great practical value for water and soil erosion management. This paper presents a new method for simulating the evolution of a gully head in a loess catchment with CA based on the Fisher discriminant. The loess catchment is an indoor, small loess watershed that was constructed in a fixed-intensity rainfall erosion test facility. The study showed that the Fisher discriminant based CA model is suitable for simulating the complex evolution process of gully head evolution in small loess watersheds. In the experiment of this study, the Fisher discriminant based CA model has two advantages. First, the Fisher discriminant can be used to calculate parameters easily and precisely. The parameters greatly affect transition probabilities and can reveal the theoretical and intuitive meaning of how spatial variables contribute to the evolution of loess gully heads. Second, the CA model is preferred for its local rules and iterative loop, which make it possible to simulate dynamic gully head evolution processes in catchments.

The transformation of the gully head spatial distribution reflects the terrain evolution in small loess catchment. In addition, each iteration result from the CA model displayed the dynamic progress of this evolution. The nearest neighbor, G-function, K-function, Moran′s I and the fractal index D were introduced to evaluate the precision of the simulated results regarding point spatial patterns, spatial autocorrelations and the fractal dimension. The comparisons between the actual and simulated point indexes proved the validity of the CA based loess gully head evolution model.

This simulation process depends on understanding geomorphological processes, especially regarding the roles that each spatial variable plays on the evolution of gully heads by analyzing the parameters that were determined with the Fisher discriminant. The research results can be used to predict the possible landform evolution trends in some loess catchments.

Table 3 Index comparison between actual and simulated gully head results

	Nearest neighbor index	Moran′s I	Box-counting method		Scale transform method	
			Fractal index (D)	Correlation coefficient	Fractal index (D)	Correlation coefficient
Actual result	0.899	0.8799	0.806	0.848	1.910	0.980
Simulated result	0.937	0.7964	0.660	0.778	1.600	0.902

References

Batty M, Xie Y, Sun Z, 1999. Modeling urban dynamics through GIS-based cellular automata. *Computers*, *Environment and Urban Systems*, 23(3): 205–233. doi: 10.1016/S0198-9715(99)00015-0

Cao M, Tang G A, Zhang Fang *et al.*, 2013. A cellular automata model for simulating the evolution of positive-negative terrains in a small loess watershed. *International Journal of Geographical Information Science*, 27(7): 1349–1363. doi: 10.1080/13658816.2012.756882

Chase C G, 1992. Fluvial landsculpting and the fractal dimension of topography. *Geomorphology*, 5(1): 39–57.

Clark P J, Evans F C, 1954. Distance to nearest neighbor as a measure of spatial relationships in populations. *Ecology*, 35(4): 445–453.

Clarke K C, Brass J A, Riggan P J, 1994. A cellular automata model of wildfire propagation and extinction. *Photogrammetric Engineering & Remote Sensing*, 60(11): 1355–1367.

Clarke K C, Gaydos L J, 1998. Loose-coupling a cellular automata model and GIS: Long-term urban growth prediction for San Francisco and Washington/Baltimore. *International Journal of Geographical Information Science*, 12(7): 699–714.

Clarke K C, Hoppen S, Gaydos L J, 1997. A self-modifying cellular automaton model of historical urbanization in the San Francisco Bay area. *Environment and Planning B*: *Planning and Design*, 24(2): 247–261.

Couclelis H, 1985. Cellular worlds: A framework for modeling micro-macro dynamics. *Environment and Planning*, A(17): 585–596.

Couclelis H, 1988. Of mice and men: What rodent populations can teach us about complex spatial dynamics. *Environment and Planning A*, 20(1): 99–109.

Couclelis H, 1989. Macrostructure and microbehavior in a metropolitan area. *Environment and planning B*, 16(2): 141–154.

Couclelis H, 1997. From cellular automata to urban models: New principles for model development and implementation. *Environment and Planning B*: *Planning and Design*, 24(2): 165–174.

Cui Lingzhou, 2002. *The Coupling Relationship Between the Sediment Yield of Rainfall Erosion and the Topographic Feature of Small Watershed on Loess Plateau*. Yangling: Institute of Soil and Water Conservation, Chinese Academy of Sciences.

Densmore A L, Ellis M A, Anderson R S, 1998. Landsliding and the evolution of normal fault-bounded mountains. *Journal of Geophysical Research*: *Solid Earth*, 103(B7): 15203–15219. doi: 10.1029/98JB00510

Gatrell A C, Bailey T C, Diggle P J *et al.*, 1996. Spatial point pattern analysis and its application in geographical epidemiology. *Transactions of the Institute of British Geographers*, 21(1): 256–274.

Gregorio S D, Serra R, 1999. An empirical method for modelling and simulating some complex macroscopic phenomena by cellular automata. *Future Generation Computer Systems*, 16(2): 259–271. doi: 10.1016/S0167-739X(99)00051-5

Haase P, 1995. Spatial pattern analysis in ecology based on Ripley's K-function: Introduction and methods of edge correction. *Journal of Vegetation Science*, 6(4): 575–582. doi: 10.2307/3236356

Hargrove W W, Gardner R H, Turner M G *et al.*, 2000. Simulating fire patterns in heterogeneous landscapes. *Ecological modelling*, 135(2): 243–263.

Howard A D, 1994. A detachment-limited model of drainage basin evolution. *Water Resources Research*, 30(7): 2261–2285. doi: 10.1029/94WR00757

Ke C Q, 2006. Modeling soil erosion in Chinese Loess Plateau using Cellular Automata. *Geoscience and Remote Sensing Symposium*, *2006. IEEE International Conference on*, 1063–1066. doi: 10.1109/IGARSS.2006.274

Li X, Liu X P, 2006. An extended cellular automaton using case-based reasoning for simulating urban development in a large complex region. *International Journal of Geographical Information Science*, 20: 1109–1136. doi: 10.1080/13658810600816870

Li X, Yeh A G O, 2000. Modelling sustainable urban development by the integration of constrained cellular automata and GIS. *International Journal of Geographical Information Science*, 14(2): 131–152. doi: 10.1080/136588100240886

Li X, Yeh A G O, 2002. Neural-network-based cellular automata for simulating multiple land use changes using GIS. *International Journal of Geographical Information Science*, 16(4): 323–343. doi: 10.1080/13658810210137004

Liu X P, Li X, Liu L *et al.*, 2008a. A bottom-up approach to discover transition rules of cellular automata using ant intelligence. *International Journal of Geographical Information Science*, 22(11–12): 1247–1269. doi: 10.1080/13658810701757510

Liu X P, Li X, Shi X *et al.*, 2008b. Simulating complex urban development using kernel-based non-linear cellular automata. *Ecological Modelling*, 211(1): 169–181. doi: 10.1016/j.ecolmodel.2007.08.024

Liu X P, Li X, Shi X *et al*., 2010. Simulating land use dynamics under planning policies by integrating artificial immune systems with cellular automata. *International Journal of Geographical Information Science*, 24(5): 783–802. doi: 10.1080/13658810903270551

Liu X P, Ma L, Li X *et al*., 2014. Simulating urban growth by integrating landscape expansion index (LEI) and cellular automata. *International Journal of Geographical Information Science*, 28(1): 148–163. doi: 10.1080/13658816.2013.831097

Liu Xiaoping, Li Xia, 2007. Fisher discriminant and automatically getting transition rule of CA. *Acta Geodaetica et Cartographica Sinica*, 36(1): 112–118. (in Chinese)

Mandelbrot B B, 1983. *The Fractal Geometry of Nature/Revised and Enlarged Edition.* New York: W.H. Freeman and Company, 495.

Moran P A P, 1950. Notes on continuous stochastic phenomena. *Biometrika*, 37(1–2): 17–23.

Murray A B, Paola C, 1994. A cellular model of braided rivers. *Nature*, 371(6492): 54–57. doi: 10.1038/371054a0

Neil G, Curtis K, 1997. Shape recognition using fractal geometry.

Pattern Recognition, 30(12): 1957–1969.

Ripley B D, 1977. Modelling spatial patterns. *Journal of the Royal Statistical Society. Series B* (*Methodological*), 39(2): 172–212.

Shi H, Shao M, 2000. Soil and water loss from the Loess Plateau in China. *Journal of Arid Environments*, 45(1): 9–20. doi: 10.1006/jare.1999.0618

Smith R, 1991. The application of cellular automata to the erosion of landforms. *Earth Surface Processes and Landforms*, 16(3): 273–281. doi: 10.1002/esp.3290160307

Tian Y, Wu L, Gao Y *et al.*, 2008. DEM-based modeling and simulation of modern landform evolution of loess. In: *Earth and Environmental Science*, *Advances in Digital Terrain Analysis*, *Lecture Notes in Geoinformation and Cartography* (*Section 3*). Berlin: Springer, 257–276.

Tucker G E, Slingerland R L, 1994. Erosional dynamics, flexural isostasy, and long-lived escarpments: A numerical modeling study. *Journal of Geophysical Research*: *Solid Earth* (*1978–2012*), 99(B6): 12229–12243.

Unwin D J, 1996. GE, spatial analysis and spatial statistics. *Progress in Human Geography*, 20(4): 540–551.

Wang Y, Zhang X, 2001. A dynamic modeling approach to simulating socioeconomic effects on landscape changes. *Ecological Modelling*, 140(1): 141–162. doi: 10.1016/S0304-3800(01)00262-9

White R, Engelen G, 1993. Cellular automata and fractal urban form: A cellular modeling approach to the evolution of urban land-use patterns. *Environment and Planning A*, 25(8): 1175–1199.

Willgoose G, 2005. Mathematical modeling of whole landscape evolution. *Annual Review of Earth and Planetary Sciences*, 33(1): 443–459. doi: 10.1146/annurev.earth.33.092203.122610

Willgoose G, Bras R L, Rodriguez-Iturbe I, 1991. Results from a new model of river basin evolution. *Earth Surface Processes and Landforms*, 16(3): 237–254. doi: 10.1002/esp.3290160305

Wu F, 2002. Calibration of stochastic cellular automata: The application to rural-urban land conversions. *International Journal of Geographical Information Science*, 16(8): 795–818. doi: 10.1080/13658810210157769

Wu F, Webster C J, 1998. Simulation of land development through the integration of cellular automata and multicriteria evaluation. *Environment and Planning B*: *Planning and Design*, 25(1): 103–126.

Yang J Y, Tang G O, Cao M *et al*., 2013. An intelligent method to discover transition rules for cellular automata using bee colony optimisation. *International Journal of Geographical Information Science*, 27(10): 1849–1864. doi: 10.1080/13658816.2013.823498

Zucca C, Canu A, Della Peruta R, 2006. Effects of land use and landscape on spatial distribution and morphological features of gullies in an agropastoral area in Sardinia (Italy). *Catena*, 68(2): 87–95. doi: 10.1016/j.catena.2006.03.015